Title
Optimal flip angle for high contrast balanced SSFP cardiac cine imaging

Journal
Magnetic Resonance in Medicine, 73(3)

ISSN
0740-3194

Authors
Srinivasan, S
Ennis, DB

Publication Date
2015-03-01

DOI
10.1002/mrm.25228

Peer reviewed

Magnetic Resonance in Medicine 73:1095–1103 (2015)

Optimal Flip Angle for High Contrast Balanced SSFP Cardiac Cine Imaging

Subashini Srinivasan[1,2] and Daniel B. Ennis[1,2,3]*

Purpose: To determine the optimal flip angle (FA) for cardiac cine imaging that maximizes myocardial signal and blood-myocardium contrast.

Methods: Bloch equation simulations of stationary myocardium and flowing blood with an imperfect slice profile were compared to in vivo measurements of blood and myocardium signal-to-noise ratio (SNR) and blood-myocardium contrast-to-noise ratio (CNR) in healthy subjects (N = 10) in the short-axis and four-chamber views and in patients (N = 7) in the three-chamber imaging plane.

Results: Left ventricular (LV) and right ventricular (RV) blood SNR and blood-myocardium CNR increases with increasing FA up to ≈105° in the short-axis view. A similar trend is seen in the RV four-chamber view, but a marked SNR difference between the LV and RV blood appears for FA>75°, especially during systole. Notable RV and LV SNR and CNR differences are also evident in the three-chamber view due to the predominant LV in-plane flow versus RV through-plane flow.

Conclusion: Very high blood-myocardium CNR can be obtained with a FA of ≈105° in the short-axis plane and ≈75° in the three-chamber and four-chamber imaging planes. However, if through-plane flow is limited, as may occur for patients with low ejection fraction or low heart rates, then the FA may be limited to ≈75°. **Magn Reson Med 73:1095–1103, 2015.**

Key words: cardiac cine imaging; balanced steady state free precession (bSSFP); optimal flip angle; maximum blood-myocardium contrast

INTRODUCTION

Cine magnetic resonance imaging (MRI) is routinely performed for the clinical assessment of cardiac structure and function using balanced steady state free precession (bSSFP) imaging. bSSFP cardiac cine imaging is preferred over conventional spoiled gradient echo (SPGR) imaging due to its high signal-to-noise ratio (SNR), high SNR efficiency, and high blood-myocardium contrast-to-noise ratio (CNR) (1,2). Conventional SPGR cardiac cine imaging largely depends on the inflow of blood to generate blood-myocardium CNR (3), whereas the blood-myocardium CNR in bSSFP imaging depends on both inflow and out-of-slice effects (4) and the tissue T_2/T_1 ratio, as well as repetition time (TR) and flip angle (FA). The strong dependence of the blood-myocardium CNR in bSSFP imaging on the T_2/T_1 ratio is especially useful for imaging patients with poor cardiac function and low blood inflow enhancement (1). The high blood-myocardium CNR in bSSFP also enables automatic myocardial segmentation (5) and improved accuracy of ventricular mass quantification (6). The SNR of bSSFP imaging is also higher than traditional SPGR techniques due to the fully refocused (i.e., balanced) gradients and balanced radio frequency (RF) phase cycling (7,8) during each pulse repetition time (TR), which enables magnetization recycling without the need for spoiling.

Maximizing both SNR and CNR are desirable as they lead to improvements in image quality that can improve diagnostic accuracy, produce images that can be automatically segmented with greater robustness, and when in excess make high acceleration rates with parallel imaging or compressed sensing judicious. Bandwidth and TR have minimal influence on the SNR and CNR of bSSFP (9) sequence. Thus, we sought to investigate the FA that produces optimal SNR and CNR for cardiac cine imaging with bSSFP with constant bandwidth and TR. Bloch equation simulations can be used to optimize the imaging parameters to produce high SNR or high blood-myocardium CNR. Previous Bloch equation simulations of stationary blood and stationary myocardium with perfect slice profiles at 1.5T and 3T indicate that the optimal FA for high blood-myocardium contrast is 54° and 42°, respectively (10); however, these values are not in good agreement with clinical experience. This is because the in vivo myocardial signal varies significantly compared to Bloch simulations with a perfect slice profile due to important dependencies on slice profile imperfections and B_0 and B_1 inhomogeneities (11). The in vivo blood signal also varies considerably due to the dependence on the imperfect slice profile, FA, flow profile, inflow effects, and out-of-slice (4,12) effects.

Therefore, our objective was to define the FAs corresponding to the maximum myocardial signal, maximum blood signal, and the maximum blood-myocardium contrast using detailed Bloch equation simulations that included the effects of imperfect slice profile, FA, inflow effects, and out-of-slice flow effects and compare these with in vivo measurements of the blood and myocardium SNR and the blood-myocardium CNR in short-axis, four-chamber, and three-chamber imaging planes. We hypothesized that the optimal FA for maximum blood-myocardium contrast was higher than 54° at 1.5T and

[1]Department of Radiological Sciences, University of California, Los Angeles, California, USA.

[2]Department of Bioengineering, University of California, Los Angeles, California, USA.

[3]Biomedical Physics Interdepartmental Program, University of California, Los Angeles, California, USA.

*Correspondence to: Daniel B. Ennis, Ph.D., Peter V. Ueberroth Building, Suite 1471, Room B, 10945 Le Conte Avenue, Los Angeles, CA 90095.
E-mail: daniel.ennis@ucla.edu

Received 23 October 2013; revised 24 January 2014; accepted 2 March 2014

DOI 10.1002/mrm.25228
Published online 2 April 2014 in Wiley Online Library (wileyonlinelibrary.com).

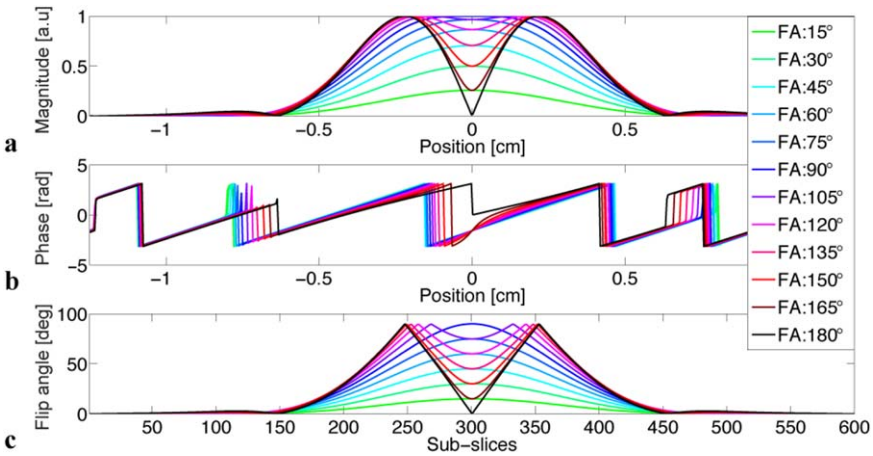

FIG. 1. The magnitude **(a)** and phase **(b)** of the slice profile of the radio frequency (RF) pulse for different flip angles 15° to 180° in steps of 15° (green to black) with respect to the slice position measured in cm. The slice profile over the imaging slice becomes poor for high flip angles due to short RF pulse duration and short bandwidth time product used for fast balanced steady state free precession cardiac cine imaging. The flip angles calculated from the slice profile for different subslices (Ns = 600) are shown in **(c)**.

was dependent on the imaging plane due to the differences in blood inflow characteristics.

METHODS

Bloch Equation Simulations

Bloch equation simulations were performed in MATLAB (The Mathworks, Natick, MA). A hamming windowed sinc RF pulse with duration = 1200 μs with a time bandwidth product = 1.6 was simulated for a range of FAs between 15° and 180° in steps of 15°. The RF pulse simulation parameters matched the in vivo image acquisition (see below). The RF pulse duration was increased to 1,200 μs compared to the conventional 1,000 μs for all the FAs to reduce the specific absorption rate (SAR) of the sequence and allow in vivo imaging at higher FA (approximately >80°). The signal characteristics of the imperfect slice profile due to the chosen RF pulse were calculated by simulating 600 subslices (N_s) within the imaging slice. A high N_s was chosen to sample the sharp transitions in the slice profile of higher FAs. The magnitude and the phase of the slice profile (Fig. 1a–1b) was determined by calculating the magnitude and phase of the transverse magnetization of the RF excitation pulse using a spinor representation of the rotations of the sampled RF pulse (13). As expected, the slice profile deteriorates for FA>90° due to the chosen pulse duration and time bandwidth product required for short TR, which is needed to reduce the off-resonance artifacts as well as the breath-hold duration. The phase of the slice profile varies linearly within the imaging slice for all the FAs except the 180°. The FA corresponding to each of the 600 subslices within the slice was determined by inverse sine of the slice profile (Fig. 1c).

One-dimensional (1D) bSSFP signal with respect to the echo number was simulated using a train of equally spaced RF pulses with identical parameters as mentioned above, with constant FA and alternating RF phase for on-resonance spins. The signal was calculated for each of the subslices with their corresponding FA, individually for each echo number. The bSSFP signal simulation parameters were TR = 4.4 ms, echo time (TE) = 2.2 ms, $N_{echoes} = 600$ and for a range of FAs between 15° and 180° in steps of 1°. The simulations were performed for stationary myocardium (T_1/T_2: 1030/40 ms) (14) and stationary blood and flowing blood ($T_1/T_2/T_2^*$: 1441/290/145 ms) (14) at 1.5 T. A longer TR and TE were used in the simulations to match the in vivo experiments (see below) to reduce the SAR of the sequence without significantly changing the contrast. The spin density of the myocardium and blood was $M_{0myo} = 0.7$ and $M_{0blood} = 0.95$ (10), respectively.

The flow simulation was performed for both blood and myocardium and followed the previous work of Markl et al. (4) with a percent spin replacement per TR (Δs) ranging from 0% (no flow) to 100%. For example, Δs = 50% and Δs = 100% corresponds to a velocity of 56.8 cm/s and 113.2 cm/s, respectively, for flowing blood or moving myocardium through a slice thickness of 5 mm and TR of 4.4 ms. The inflow effects were simulated by replacing Δs spins within the imaging slice (N_s), with full magnetization every TR assuming a unidirectional steady plug flow of fresh blood or myocardium. The out-of-slice flow effects were simulated by tracking up to number of out-of-slice, $N_{os} = 3 \times \Delta s \times N_s \times T_2^*/TR$, subslices outside the imaging slice until their signal decayed by T_2* effects. The bSSFP signal was calculated individually for all the N_s and N_{os} subslices every TR as the absolute value of the transverse signal. Thus, the calculated signal included effects of both inflow and out-of-slice flow effects. The steady state bSSFP signal was calculated as the average signal of all the N_s and N_{os} subslices of the last echo (600th TR).

Simulations of stationary myocardium, stationary blood, and flowing blood with Δs = 50% were also performed with different off-resonances ranging from 15° to 180° in steps of 15°. Identical simulations of stationary myocardium (T_1/T_2:1471/47 ms), stationary blood, and flowing blood ($T_1/T_2/T_2^*$:1932/275/138 ms) with perfect and imperfect slice profiles were simulated for

comparison of the optimal FA required for high blood-myocardium contrast at 3T. The signal increases as B_0^2 and hence to compare the myocardium and blood signal with 1.5T, the M_0 of the blood and myocardium at 3T were scaled by 4, resulting in $M_{0myo} = 2.8$ and $M_{0blood} = 3.8$.

In Vivo Imaging Experiments

Our institutional review board approved the protocol. All images were acquired on a 1.5T scanner (Avanto; Siemens Medical Solutions, Erlangen, Germany) using a six-channel anterior cardiac coil and six-channel posterior spine matrix.

A 2D breath-hold cardiac exam was performed in 10 normal subjects (N = 10; 9 male; age: 28 ± 3 years) subsequent to obtaining informed written consent. 2D segmented, retrospectively electrocardiogram gated, midventricular short-axis and four-chamber cardiac cine images were acquired using bSSFP with FAs of 15° to 180° in 15° steps. The highest FA (180°) was not acquired in six subjects due to SAR limitations. The imaging parameters were as follows: field of view = 380 × 296 mm, acquisition matrix = 256 × 200, resolution = 1.5 × 1.5 × 5 mm, TE/TR = 2.2/4.4 ms, bandwidth = 501 Hz/px, views-per-segment = 14–16, retrospectively interpolated $N_{phases} = 20$, and 1200 μs windowed sinc RF pulse with a time bandwidth product of 1.6. The RF pulse duration was increased to 1200 μs compared to the conventional 1000 μs for all the acquisitions to reduce the SAR of the sequence and allow imaging at higher FA (approximately >80°). The bandwidth was decreased, which increases the TE and TR without significantly changing the contrast and permitted the use of higher FAs within SAR restrictions. Parallel imaging was not used in order to simplify the SNR comparison. The individual acquisition duration depended on the heart rate during the image acquisition and averaged 12 ± 1s.

Cardiac cine images were also acquired in seven patients (N = 7; 4 male; age: 32 ± 12years) in the three-chamber left ventricular outflow tract (LVOT) plane with bSSFP and FAs of 45°, 75°, and 105°—in addition to a short-axis stack bSSFP cine images that were used to measure ejection fraction. The imaging parameters were identical to those used in the healthy subjects.

In Vivo Data Analysis

The SNR of the interventricular septum, the right ventricular (RV) blood, and LV blood were measured using regions of interest analysis. The mean signal intensity within septal and RV and LV ROIs was calculated for each systolic phase (at ≈30% of the cardiac cycle) and each diastolic phase (≈90% of the cardiac cycle) for both slice orientations and for each individual. The standard deviation (SD) of the background noise was also measured within a region outside the body that was free of any artifacts. The SNR was calculated as the ratio of the mean signal to the SD of the background noise. The SNR was divided by a correction factor (15) of $\sqrt{\frac{2}{4-\pi}} = 1.53$, to account for the Rayleigh distribution of the noise. The CNR was calculated as the SNR difference between the RV or LV blood and the septum. SNR and CNR calculations for RV and LV blood and myocardium were also performed in the LVOT plane for each patient. The LV ejection fraction was calculated subsequent to manual contouring of the multi-slice short-axis acquisition for each patient by an experienced MRI technologist.

Comparison of the Bloch Simulation and Measured Data

The stationary myocardial and flowing blood signal (Δs = 50%) simulation were collectively scaled to best fit the experimentally measured septal, RV blood, and LV blood SNR for the short-axis and four-chamber views in healthy subjects based on a linear least squares fit between all the simulations and the mean experimental SNR. The stationary myocardial signal simulation was chosen because the average velocity is zero for the periodic myocardial motion. The root mean square error (RMSE) was calculated for the septum, LV blood, and RV blood. The RMSE was calculated as the square root of the ratio of the sum of squares of the differences between the fitted simulations and the measured values to the number of experiments with different FAs. The coefficient of variation of the RMSE was calculated for the septum, LV blood, and RV blood as the ratio of the RMSE to the mean of simulated and the experimental values.

RESULTS

Simulations

The Bloch simulation results for myocardium and blood for a range of FAs with different flow velocities and a perfect slice profile are shown in Figure 2a–2b. At 1.5T, the maximum stationary myocardium signal was 0.07 and occurred at a FA of 22°; the maximum stationary blood signal was 0.22 and occurred at a FA 48°; and the maximum stationary blood-myocardium signal difference (i.e., contrast) was 0.18 and occurred at a FA of 55°, which is in agreement with Schär et al. (10). In the presence of through-plane flow (Δs>0) with a perfect slice profile, the maximum flowing blood signal, the maximum moving myocardial signal, and the maximum contrast between stationary myocardium and flowing blood occurred at a FA of 90°. At 3T with a perfect slice profile, the maximum stationary myocardium signal was 0.28 and occurred at a FA of 20°; the maximum stationary blood signal was 0.8 and occurred at a FA of 42°; and the maximum stationary blood-myocardium contrast was 0.15 and occurred at a FA of 47°.

Figure 2d–2f highlight the importance of incorporating an imperfect slice profile for simulating the signal response of myocardium and blood. The maximum stationary myocardial signal occurred at 45°, the maximum stationary blood signal occurred at 135°, and the maximum contrast of 0.08 between stationary myocardium and stationary blood with imperfect slice profile occurred at 135°. For moving myocardium with an imperfect slice profile, the maximum myocardial signal occurred in the FA range of 105° to 120°. For flowing blood (Δs>0%) with an imperfect slice profile, the contrast between stationary myocardium and flowing blood increases to a range of 0.21 to 0.17 for a FA of 105° to 120°, and

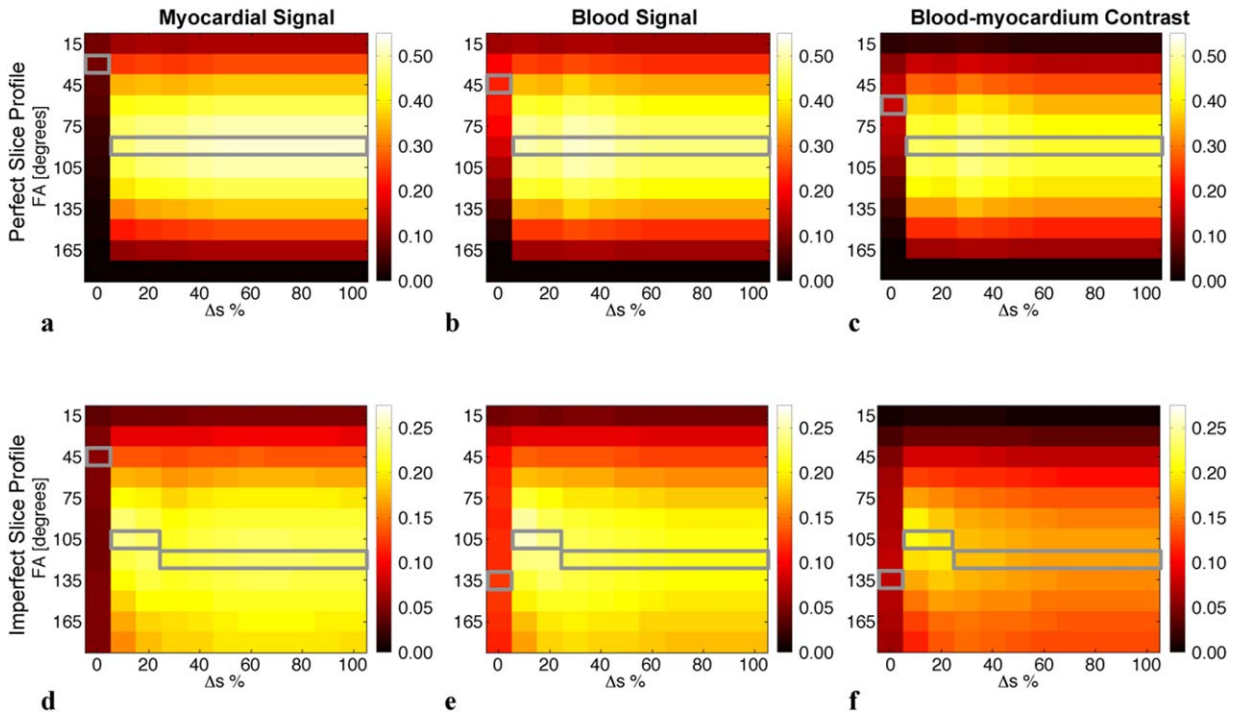

FIG. 2. Bloch simulations with perfect slice profile of myocardium **(a)** and blood **(b)** with different spin replacements per repetition time (Δs) ranging from 0% (stationary) to 100% (complete replacement of spins within the imaging slice). The contrast between blood with different Δs and stationary myocardium is shown in **(c)**. Identical signal simulations of myocardium **(d)**, blood **(e)** and blood-myocardium contrast **(f)** were performed with imperfect slice profile. Note that the scale of the bottom row figures is half the scale of the top row figures. The solid gray border indicates the maximum signal for each Δs.

thereafter decreases slightly. At 3T with an imperfect slice profile, the maximum stationary myocardial signal occurred at 30°, the maximum stationary blood signal occurred at 135°, and the maximum flowing blood signal occurred for a FA of 105° to 120°.

The influence of off-resonance on the signals for stationary myocardium, stationary blood, and flowing blood ($\Delta s = 50\%$) with an imperfect slice profile is shown in Figure 3a–3c. For flowing blood, the signal increases with both increasing off-resonance and increasing FA with an increase in the signal up to $\approx 13.9 \cdot M_0$ with 180° off-resonance, which accords with the values reported by Markl et al (4). The flowing and stationary blood signal, however, is weakly dependent on off-resonances less than 90°.

In Vivo Analysis in Healthy Subjects

Figure 4a shows a subset of the acquired diastolic and systolic short-axis cardiac images for a healthy subject with flip angles ranging from 15° to 165° in steps of 30°. The mean and SD of the SAR calculated over the 10 subjects is reported in Figure 4a. Images from 10 subjects were used to report the measured LV blood, RV blood, and myocardial SNR—as well as the LV blood-myocardium CNR and RV blood-myocardium CNR for diastolic and systolic phase, as shown in Figure 4b–4e. The myocardial SNR increases up to 30° in diastolic phase and up to 45° in systolic phase, and slightly decreases with increasing FA. The in vivo LV blood and RV blood SNR and the LV and RV blood-myocardium CNR increase with increasing FA. The LV and RV blood SNR and CNR are similar to each other in the systolic phase for all FAs, and minimal differences in their SNRs are apparent for FA>105° in the diastolic phase. The RMSE coefficient of variation between the simulated flowing blood and the mean in vivo LV blood SNR is 0.15 during diastole, 0.23 during systole, and 0.21 in the RV blood during diastole and systole. The RMSE coefficient of variation between stationary myocardium and the in vivo septal SNR is 0.27 during diastole and 0.33 during systole.

Figure 5a shows a subset of the acquired diastolic and systolic four-chamber cardiac images for a healthy subject with FAs ranging from 15° to 165° in steps of 30°. The mean and SD of the SAR calculated over the 10 subjects is reported in Figure 5a. The measured LV blood and RV blood and myocardial SNR, LV, and RV blood-myocardium CNR in the diastolic and systolic phases is shown in Figure 5b–5e, respectively. The myocardial SNR increases up to 30° in diastolic phase and up to 45° in systolic phase, and it slightly decreases with increasing FA similar to the short-axis images. The RV blood SNR and RV blood-myocardium CNR during systolic and diastolic phases is similar to the short-axis plane. However, the LV blood SNR and LV blood-myocardium CNR increases for increasing FA up to ≈75° and remains relatively constant for FA>75°. Consequently, the difference in SNR and CNR between the LV blood and RV blood increases with increasing FA and is more evident in the systolic phase (Fig. 5c, 5e) than in the diastolic phase (Fig. 5b, 5d). The coefficient of variation of the RMSE between the simulated flowing blood and the mean measured LV blood signal is 0.31 during diastole and

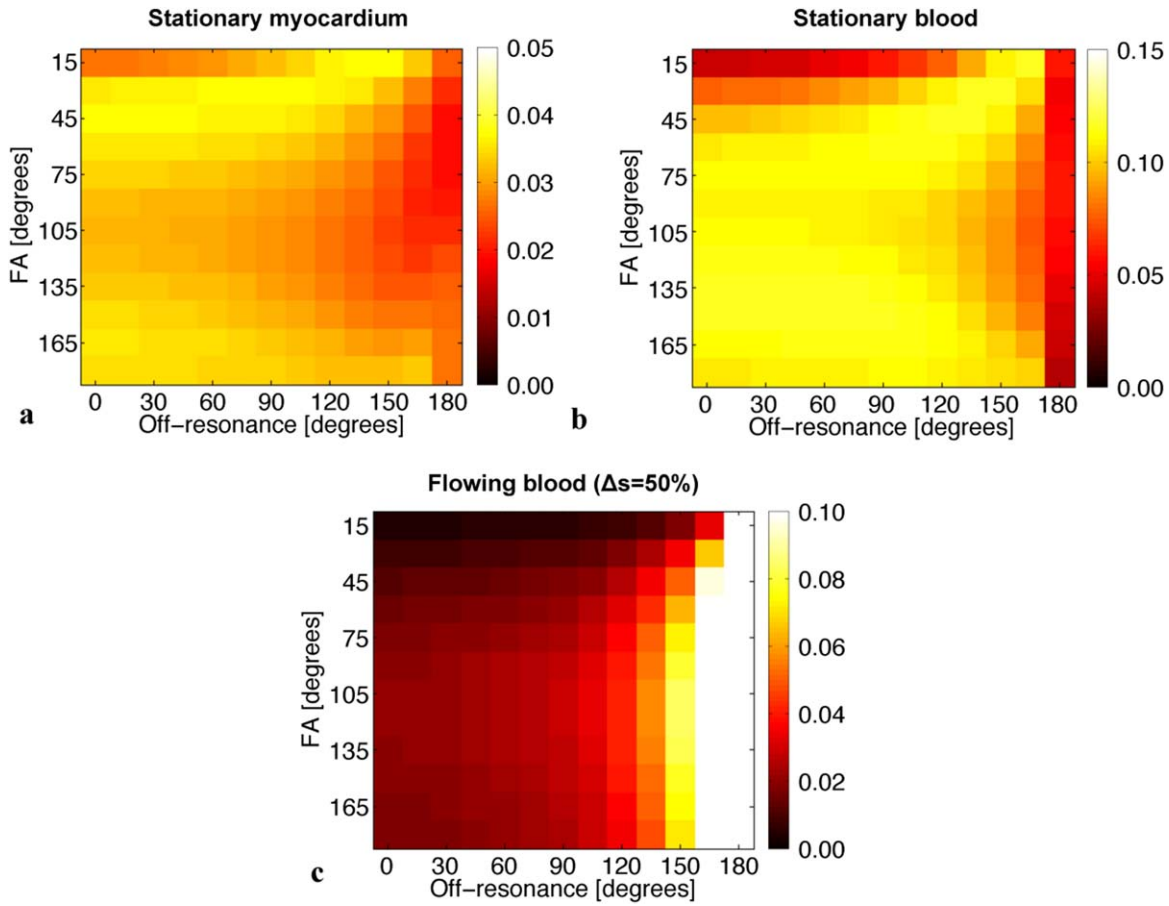

FIG. 3. Bloch simulations of stationary myocardium **(a)**, stationary blood **(b)**, and flowing blood with $\Delta s = 50\%$ **(c)** and different off-resonance in degrees along the *x*-axis. Note that the scale of the (b) and (c) are three times and ten times respectively that of the scale of (a).

0.47 during systole. The coefficient of variation of the RMSE for the RV blood signal is 0.11 during diastole and 0.17 during systole. The RMSE coefficient of variation between stationary myocardium and the in vivo septal SNR is 0.22 during diastole and 0.24 during systole.

In Vivo Analysis in Patients

The ejection fraction (EF) and heart rate of the patient during cardiac cine acquisition in part determine the flow of blood within and through the imaging plane. Figure 6a compares systolic images in the LVOT plane for two patients with similar heart rates (74 vs. 77 beats/min) but different EF (37.1% vs. 58.4%) acquired with $FA = 45°$, 75°, and 105°. The LV blood-myocardium CNR and RV blood-myocardium CNR measured during systole and diastole are shown in Figure 6b–6c. The CNR for FAs of 75° and 105° is higher than the CNR with FA of 45° in all the patients. However, there is minimal difference between the LV blood-myocardium CNR for FAs of 75° and 105° in patients with low EF or low heart rate.

DISCUSSION

In the short-axis view the measured in vivo LV and RV blood SNR in both the systolic and diastolic phases increases with increasing imaging FA. The percent increase in SNR is >10% for every 15° increase in FA over the range of 15° to 105° and decreases with further increase in FA. Bloch simulations of flowing blood and stationary myocardium signal that use an imperfect slice profile and account for out-of-slice flow effects corroborate this finding and indicate that the blood signal increases with increasing FA up to ≈105° to 120° and decreases slightly thereafter; whereas the stationary myocardial signal is relatively constant over a wide range of FAs ($>= 45°$). Thus, to achieve the highest blood-myocardium contrast cardiac cine imaging in the short-axis plane within SAR constraints, the highest possible FA up to 105°to 120° should be used.

For the four-chamber view, the measured RV blood SNR in both systolic and diastolic phases is similar to the simulated flowing blood signal and similar to the LV and RV blood SNR in the short-axis plane. However, at higher FAs (>75°), the four-chamber LV blood SNR and CNR is lower than the RV blood SNR and CNR. This likely arises as a consequence of the saturation of the blood signal in the pulmonary tissue and veins within the imaging plane that drain into the left chambers of the heart. This saturation leads to reduced in-flow effects and diminished blood signal intensity in the left chambers of the heart. Similarly, in the LVOT view, the RV blood flows predominantly through-plane compared to

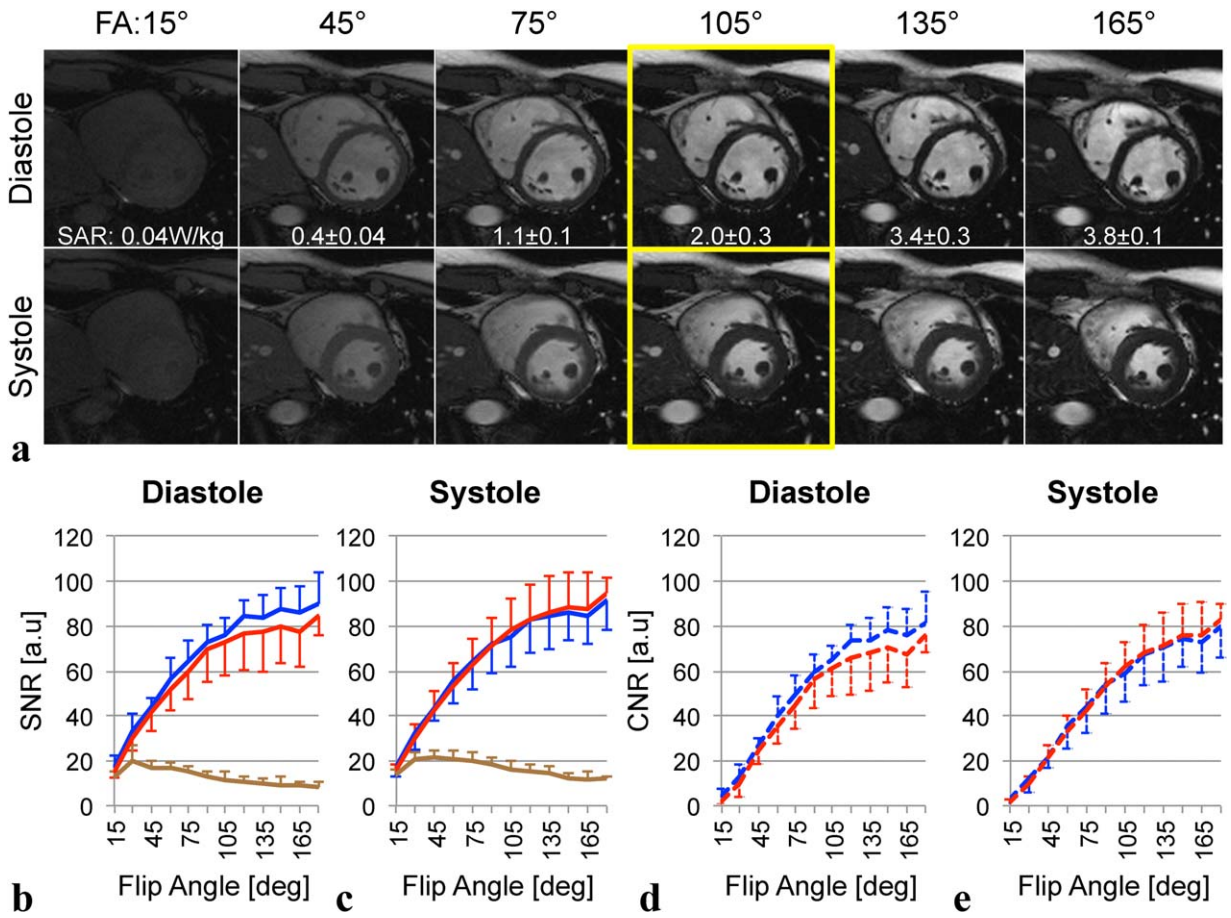

FIG. 4. **(a)** Diastolic (top row) and systolic (bottom row) images of short-axis balanced steady state free precession cardiac cine images of a healthy subject with different flip angles (FAs) from 15° to165° in steps of 30°. The mean signal-to-noise ratio (SNR) of left ventricular (LV) blood (red), right ventricular RV blood (blue), and myocardium (brown) measured during diastole **(b)** and systole **(c)**, and LV blood myocardial contrast-to-noise ratio (CNR) (red dashed) and RV blood myocardial CNR (blue dashed) during diastole **(d)** and systole **(e),** show that the blood SNR and blood-myocardium CNR increases with increasing FA, but the increase in blood SNR and CNR for FA $>$ 105° is minimal.

the LV blood flow, which largely circulates in-plane. As a consequence, the RV blood signal is noticeably higher than the LV blood signal for FA = 105° in patients with normal EF or high heart rate.

To summarize, high SNR short-axis cardiac cine images can be acquired with FAs as high as 105° to 120°, beyond which the SNR gains are limited and SAR becomes problematic. The SNR gain between FA = 75° and FA = 105° in part depends on the EF and heart rate of the patient and may be limited in patients with low EF and/or low HR (Fig. 6b–6c). Images in the four-chamber view and three-chamber view have high and uniform blood SNR in both the RV and LV up to 75°, beyond which there are increased signal differences between the RV and LV blood that may be undesirable. Bloch simulations and measured diastolic LV blood in the four-chamber plane indicate that a FA of 75° will increase the blood-myocardium CNR (by ≈21%) compared to the previously reported optimal FA of 54°. Similarly, for 3D cardiac cine applications where the blood signal is reduced due to signal saturation (16), a higher FA up to 75° is necessary to improve the blood-myocardium contrast. Simulations of stationary blood with imperfect slice profile (Fig. 2e) suggest that increasing FA beyond 75° up to 135° will only incrementally increase the blood-myocardium contrast, but it will incur substantially higher SAR.

Cardiac cine imaging, however, may be SAR-limited as the FA approaches 105°, especially with a short TR. Variable FA cardiac cine imaging (17) can be used to lower the SAR of the sequence, while maintaining the use of an effectively higher FA in order to obtain increased blood-myocardium contrast in the short-axis plane. Parallel imaging techniques such as generalized autocalibrating partially parallel acquisitions (18) and sensitivity encoding (19) can also be used to reduce the acquisition duration—and thus reduce the overall SAR of the imaging sequence, which then permits the use of a higher FA.

The flowing blood signal was simulated for a range of velocity up to 116 cm/s and was relatively independent of the through plane velocity. This accounts for the apparent blood-signal homogeneity in vivo for which a wide range of velocities are present. The optimal FA was higher for simulations using imperfect slice profiles (FA of 105° to 120°) compared to perfect slice profiles

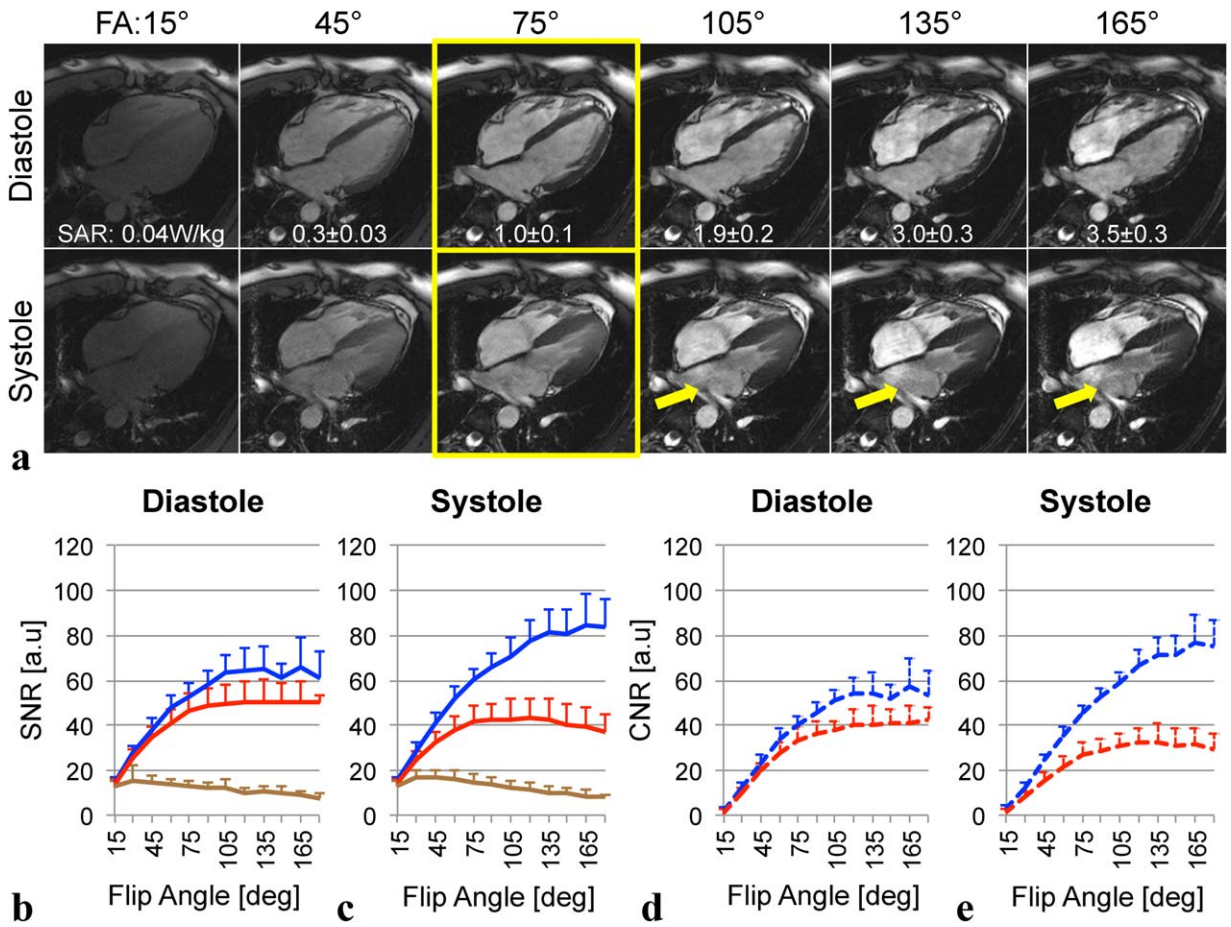

FIG. 5. **(a)** Diastolic (top row) and systolic (bottom row) images of four-chamber balanced steady state free precession cardiac cine images from a healthy subject with different flip angles (FAs) from 15° to 165° in steps of 30°. The mean signal-to-noise ratio (SNR) of left ventricular (LV) blood (red), right ventricular (RV) blood (blue), and myocardium (brown) measured during diastole **(b),** and systole **(c)** LV blood myocardial contrast-to-noise ratio (CNR) (red dashed) and RV blood myocardial CNR (blue dashed) during diastole **(d)** and systole **(e)** indicate that at higher FAs, the blood signal is decreased in the LV compared to the RV due to the blood signal saturation of the pulmonary veins with long acquisition durations. Blood SNR and blood-myocardium CNR differences are clearly visible in the systolic phase (arrows) at higher FAs (a) and measured LV and RV mean blood SNR and blood-myocardium CNR (c,e).

(FA = 90°) due to the reduction in the average FA within the imperfect slice profile despite the same nominal FA. In the flow simulations with an imperfect slice profile, it is apparent that the prescribed FA had to be increased beyond 90° in order to achieve the maximum signal by way of increasing the average FA. For the chosen RF pulse (see Methods), the highest average FA within the imaging slice was 79.3°, which occurred at the prescribed FA of 105°.

The RMSE coefficient of variations in the short-axis imaging plane between the simulation and the in vivo LV and RV blood was in the range of (0.15–0.23). The higher values were due to the inconsistency between the simulation and the in vivo values at high FA (>135°), where the simulation indicated a slight reduction in the signal and the in vivo results suggested an increase in the signal. In the four-chamber imaging plane, the RMSE coefficient of variations between the simulated flowing blood and the mean in vivo SNR for the LV blood (0.31–0.47) was higher than that of the RV blood (0.11–0.17), which was likely due to the inflow saturation of the LV blood from the pulmonary veins—an effect that was not simulated. However, the RMSE coefficient of variations between stationary blood simulation and mean LV blood was 0.08 during systole and 0.14 during diastole, suggesting that the lower in vivo SNR was partly due to blood signal saturation as a consequence of in-plane flow. The RMSE coefficient of variations for the myocardium was high (0.22–0.33) in both four-chamber and short-axis imaging planes. This was partly due to the stationary myocardial signal simulation with imperfect slice profile (Fig. 3a), which has a nearly constant signal for FA>45°, whereas the in vivo myocardial SNR decreases with increasing FA for FA>90°. However, the stationary myocardium simulations with off-resonance indicated that the signal decreases at higher FAs for increased off-resonance, which were not considered in the RMSE calculation due to lack of the B_0 map.

The simulations were based on sinc RF pulses with a pulse duration and time bandwidth product matched to the parameters of the product sequence. As a consequence, the slice profile for each different FA was suboptimal. The RF

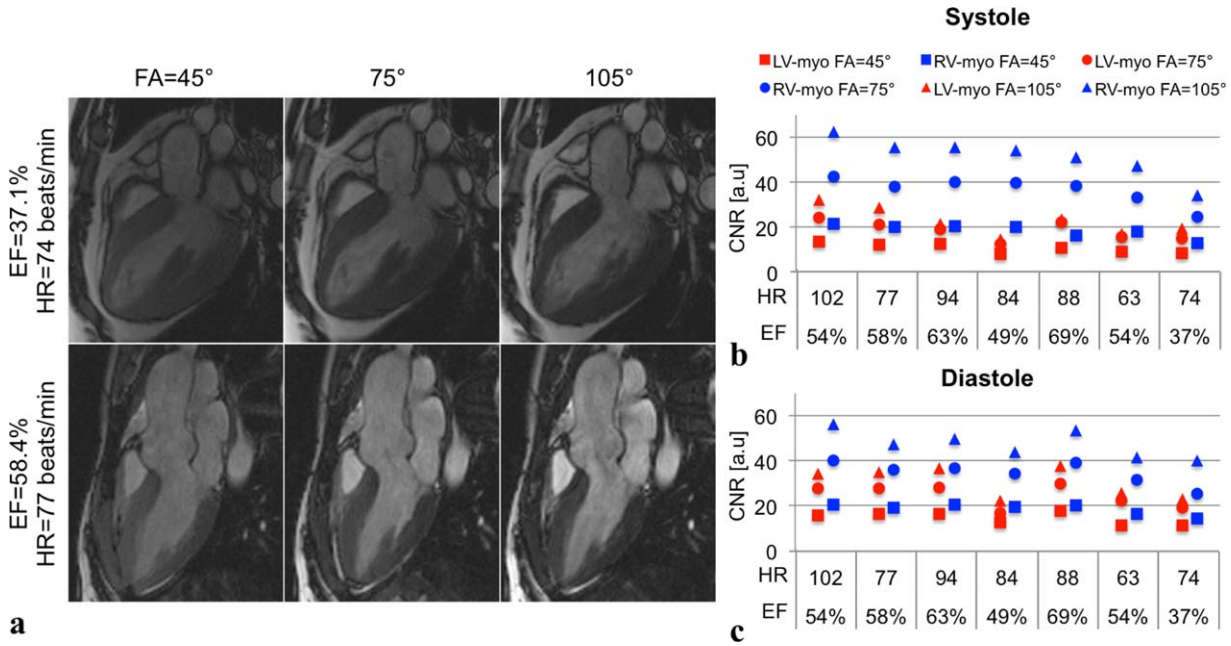

FIG. 6. **(a)** Three-chamber left ventricular outflow tract images of two different patients with (top) low ejection fraction (EF) = 37.1% and (bottom) normal EF = 58.4% and similar heart rates (HR) of 74 vs. 77 beats/min acquired at flip angles = 45°, 75°, and 105°. The LV blood-myocardium contrast-to-noise ratio (CNR) (red) and right ventricular (RV) blood-myocardium CNR (blue) were measured in seven patients at FA = 45° (square), 75° (circle), and 105° (triangle) during systole **(b)** and diastole **(c)**. RV blood-myocardium CNR exceeds LV blood-myocardium CNR due to the differences in through-plane versus in-plane flow. CNR values also tend to be lower for subjects with low EF and/or low HR.

pulses for different FAs can be individually optimized for their slice profile and SAR using Shinnar-Le Roux (13) and variable rate selective excitation (20,21) pulse design, which will reduce the optimal FA results to more closely align with the simulations that used a perfect slice profile.

Limitations

The TR of the imaging sequence was specifically increased to 4.4 ms to reduce the SAR and enable imaging at high FAs. In practice, the TR of the imaging sequence is minimized to reduce sensitivity to B_0 inhomogeneities and the related banding artifacts for bSSFP cardiac cine imaging. Our simulations and preliminary experiments in five healthy subjects with FA up to 80° and TR = 3.1 ms (data not reported) demonstrated a similar trend in the myocardial and blood signal compared to those acquired with TR = 4.4 ms. The myocardial and blood signals at TR = 3.1 ms, however, were slightly higher than at TR = 4.4 ms but did not shift the optimal FA. Nevertheless, the use of a high FA is preferred to increase blood-myocardium contrast when possible, while staying within SAR limits.

The flow simulations considered only in-flow effects due to through plane flow. Further improvements to these simulations are required to incorporate the periodic motion of the myocardium and to define the optimal FA for the myocardium. The differences in the blood signal between the LV and the RV blood as well as between the different cardiac phases and different imaging planes are due to the flow effects such as in-plane flow and blood signal saturation due to recirculating spins. Further improvements to the flowing blood simulations would be required to account for these patient specific flow effects.

CONCLUSION

Bloch equation simulations of flowing blood and stationary myocardium with an imperfect slice profile agree well with the measured blood-myocardium CNR in the short-axis and four-chamber imaging planes in healthy subjects. High blood-myocardium CNR can be obtained with a FA ≈105° when imaging a plane with predominantly through-plane flow such as the short-axis plane and increasing the FA beyond 105° results in limited SNR and CNR gains compared to the quadratic increases in SAR. When imaging planes with both through-plane flow and in-plane flow such as the four-chamber and three-chamber imaging planes, the maximum FA should be limited to ≈75° if uniform blood SNR is desired in both the LV and RV. Finally, the FA may similarly be limited to ≈75° if through-plane flow is limited, as may occur for patients with low ejection fraction or low heart rates.

ACKNOWLEDGMENT

This work was supported in part by funding from the American Heart Association and Siemens Medical Solutions to DBE. The authors would like to thank Dr. J Paul Finn, Sergio Godinez, Francine Cobla, and Karen Mae Hernandez for acquiring the patient data.

REFERENCES

1. Finn JP, Nael K, Deshpande V, Ratib O, Laub G. Cardiac MR imaging: state of the technology. Radiology 2006;241:338–354.

2. Barkhausen J, Ruehm SG, Goyen M, Buck T, Laub G, Debatin JF. MR evaluation of ventricular function: true fast imaging with steady-state precession versus fast low-angle shot cine MR imaging: feasibility study. Radiology 2001;219:264–269.
3. Laub GA. Time-of-flight method of MR angiography. Magn Reson Imaging Clin N Am 1995;3:391–398.
4. Markl M, Pelc NJ. On flow effects in balanced steady-state free precession imaging: pictorial description, parameter dependence, and clinical implications. J Magn Reson Imaging 2004;20:697–705.
5. Francois CJ, Fieno DS, Shors SM, Finn JP. Left ventricular mass: manual and automatic segmentation of true FISP and FLASH cine MR images in dogs and pigs. Radiology 2004;230:389–395.
6. Shors SM, Fung CW, Francois CJ, Finn JP, Fieno DS. Accurate quantification of right ventricular mass at MR imaging by using cine true fast imaging with steady-state precession: study in dogs. Radiology 2004;230:383–388.
7. Scheffler K. A pictorial description of steady-states in rapid magnetic resonance imaging. Concept Magn Reson 1999;11:291–304.
8. Scheffler K, Lehnhardt S. Principles and applications of balanced SSFP techniques. Eur Radiol 2003;13:2409–2418.
9. Reeder SB, Herzka DA, McVeigh ER. Signal-to-noise ratio behavior of steady-state free precession. Magn Reson Med 2004;52: 123–130.
10. Schär M, Kozerke S, Fischer SE, Boesiger P. Cardiac SSFP imaging at 3 Tesla. Magn Reson Med 2004;51:799–806.
11. Sung K, Lee HL, Hu HH, Nayak KS. Prediction of myocardial signal during CINE balanced SSFP imaging. Magma 2010;23:85–91.
12. Markl M, Alley MT, Elkins CJ, Pelc NJ. Flow effects in balanced steady state free precession imaging. Magn Reson Med 2003;50:892–903.
13. Pauly J, Le Roux P, Nishimura D, Macovski A. Parameter relations for the Shinnar-Le Roux selective excitation pulse design algorithm [NMR imaging]. IEEE Trans Med Imaging 1991;10:53–65.
14. Stanisz GJ, Odrobina EE, Pun J, et al. T1, T2 relaxation and magnetization transfer in tissue at 3T. Magn Reson Med 2005;54:507–512.
15. Dietrich O, Raya JG, Reeder SB, Reiser MF, Schoenberg SO. Measurement of signal-to-noise ratios in MR images: influence of multichannel coils, parallel imaging, and reconstruction filters. J Magn Reson Imaging 2007;26:375–385.
16. Nezafat R, Herzka D, Stehning C, Peters DC, Nehrke K, Manning WJ. Inflow quantification in three-dimensional cardiovascular MR imaging. J Magn Reson Imaging 2008;28:1273–1279.
17. Srinivasan S, Ennis DB. Variable flip angle balanced steady-state free precession for lower SAR or higher contrast cardiac cine imaging. Magn Reson Med 2014;71:1035–1043.
18. Griswold MA, Jakob PM, Heidemann RM, et al. Generalized autocalibrating partially parallel acquisitions (GRAPPA). Magn Reson Med 2002;47:1202–1210.
19. Pruessmann KP, Weiger M, Scheidegger MB, Boesiger P. SENSE: sensitivity encoding for fast MRI. Magn Reson Med 1999;42(5):952–962.
20. Conolly S, Nishimura D, Macovski A, Glover G. Variable-rate selective excitation. J Magn Reson (1969) 1988;78:440–458.
21. Hargreaves BA, Cunningham CH, Nishimura DG, Conolly SM. Variable-rate selective excitation for rapid MRI sequences. Magn Reson Med 2004;52:590–597.